Quark-model identification of baryon ground and resonant states

T. Melde, W. Plessas, and B. Sengl

Theoretische Physik, Institut für Physik, Karl-Franzens-Universität, Universitätsplatz 5, A-8010 Graz, Austria

We present a new classification scheme of baryon ground states and resonances into $SU(3)$ flavor multiplets. The scheme is worked out along a covariant formalism with relativistic constituent quark models and it relies on detailed investigations of the baryon spectra, the spin-flavor structure of the baryon eigenstates, the behavior of their probability density distributions as well as covariant predictions for mesonic decay widths. The results are found to be quite independent of the specific types of relativistic constituent quark models employed. It turns out that a consistent classification requires one to include also resonances that are presently reported from experiments with only two-star status.

I. INTRODUCTION

Recently a comprehensive study of hadronic decays of baryon resonances along relativistic constituent quark models (RCQMs) has become available. In particular, one considered the π, η, and K decay modes in the light and strange baryon sectors [1–3]. The calculations were done within the framework of relativistic quantum mechanics, specifically in the point form. The covariant quark-model predictions were found to be drastically different from results of previous nonrelativistic or relativized calculations as, e.g., in Refs. [4–9]. The relativistic results for partial decay widths systematically underestimate the available experimental data. Similar results for hadronic decay widths with practically the same characteristics were also seen in another relativistic study [10,11]. This is remarkable, since the latter investigation was carried out along a completely different approach using the Bethe-Salpeter equation [12,13].

The observed systematics of the relativistic results for decay widths has suggested to revisit the identification of quark-model eigenstates with established baryon resonances [14]. For instance, it was found that in the Σ spectrum the lowest $J^P = \frac{1}{2}^-$ state should not be identified with the $\Sigma(1750)$ resonance, which is established at three-star status, but rather with the $\Sigma(1560)$ resonance [2]. The latter is often neglected because it is reported only as a two-star resonance without a J^P assignment [15].

Evidently, it is not enough to consider only energy levels to reach a conclusive classification of baryon resonances. Rather one should take into account also properties relating to the resonance structure such as decay widths. Theoretically one can examine the detailed spin and flavor contents as well as the spatial symmetries of all resonance states, since their wave functions are directly accessible. This leads to a consistent identification of states along $SU(3)$ flavor multiplets. The present work is essentially devoted to a comprehensive investigation of the multiplet classification within a covariant formalism along RCQMs. In several cases this yields results different from what is

understood as the usual quark-model classification. In addition, the inclusion of low-lying resonances with less than three-star status turns out to be necessary.

It is mandatory to work within a relativistic framework. Obviously, the constituent quarks confined to a finite volume carry high momenta. Large relativistic effects are present in all aspects of baryon states, as was found in covariant studies of electroweak nucleon form factors [12,16–20], electric radii as well as magnetic moments [10,21], and mesonic decays [1–3,10,11]. For the relativistic description we use the formalism of Poincaré-invariant quantum mechanics [22]. The theory relies on a relativistically invariant mass operator, and it allows one to incorporate all symmetries required by special relativity. Different forms of relativistic quantum mechanics are characterized by different kinematical subgroups of the Poincaré group. The most common ones are the instant, front, and point forms [23,24]. Here we adhere to the point form.

In the following section we shortly outline the theoretical framework and describe the specific RCQMs used. The third section deals with the baryon excitation spectra as produced by the RCQMs. Then we discuss the mesonic decays of the established baryon resonances in comparison to the available experimental data. In the fifth section we identify the theoretical eigenstates with the phenomenologically known resonances and propose a new classification scheme for baryon ground and resonant states. There, also the spin-flavor structures as well as spatial density distributions of the various flavor-multiplet members are detailed. Subsequently we discuss their decay properties and end with our conclusions.

II. RELATIVISTIC QUARK MODELS

Here we formulate the Poincaré-invariant description of baryon eigenstates. Following the point form of relativistic quantum mechanics we outline the eigenvalue problem of the invariant mass operator and specify the dynamics of two different types of RCQMs.

A. Eigenvalue problem of the invariant mass operator

Starting out from the free mass operator $\hat{M}_{\text{free}}$ the interactions are introduced according to the Bakamjian-Thomas construction [25]. Thus the free mass operator is replaced by a full mass operator $\hat{M}$ containing an interacting term $\hat{M}_{\text{int}}$

$$\hat{M}_{\text{free}} \rightarrow \hat{M} = \hat{M}_{\text{free}} + \hat{M}_{\text{int}}. \tag{1}$$

For a given baryon state of mass M and total angular momentum (intrinsic spin) J with z projection Σ the eigenvalue problem of the mass operator reads

$$\hat{M}|V, M, J, \Sigma\rangle = M|V, M, J, \Sigma\rangle. \tag{2}$$

Here we have written the eigenstates in obvious notation as $|V, M, J, \Sigma\rangle$, where V indicates the four eigenvalues of the velocity operator $\hat{V}^\mu$, of which only three are independent.

The four-momentum operator is then defined by multiplying the mass operator $\hat{M}$ by the four-velocity operator

$$\hat{P}^\mu = \hat{M}\hat{V}^\mu, \tag{3}$$

and it becomes interaction-dependent. Alternatively we can thus express the baryon eigenstates also as

$$|V, M, J, \Sigma\rangle \equiv |P, J, \Sigma\rangle, \tag{4}$$

where P represents the four eigenvalues of $\hat{P}^\mu$, whose square gives the invariant mass operator.

The ground and resonance state wave functions are defined through the velocity-state representations of the mass-operator eigenstates

$$\langle v; \vec{k}_1, \vec{k}_2, \vec{k}_3; \mu_1, \mu_2, \mu_3 | V, M, J, \Sigma \rangle$$
$$= \frac{\sqrt{2}}{M} v_0 \delta^3(\vec{v} - \vec{V}) \sqrt{\frac{2\omega_1 2\omega_2 2\omega_3}{(\omega_1 + \omega_2 + \omega_3)^3}} \Psi_{MJ\Sigma}(\vec{k}_i; \mu_i), \tag{5}$$

and they are normalized to unity as

$$\delta_{MM'}\delta_{JJ'}\delta_{\Sigma\Sigma'} = \sum_{\mu_1\mu_2\mu_3} \int d^3k_2 d^3k_3 \Psi^\star_{M'J'\Sigma'}(\vec{k}_i; \mu_i)$$
$$\times \Psi_{MJ\Sigma}(\vec{k}_i; \mu_i). \tag{6}$$

The velocity states build a specific basis of free three-body states defined by

$$|v; \vec{k}_1, \vec{k}_2, \vec{k}_3; \mu_1, \mu_2, \mu_3\rangle$$
$$= U_{B(v)}|k_1, k_2, k_3; \mu_1, \mu_2, \mu_3\rangle$$
$$= \sum_{\sigma_1,\sigma_2,\sigma_3} \prod_{i=1}^3 D^{1/2}_{\sigma_i\mu_i}[R_W(k_i, B(v))]|p_1, p_2, p_3; \sigma_1, \sigma_2, \sigma_3\rangle. \tag{7}$$

Here $B(v)$, with unitary representation $U_{B(v)}$, is a boost with four-velocity v on the free three-body states

$|k_1, k_2, k_3; \mu_1, \mu_2, \mu_3\rangle$ in the center-of-momentum system, i.e., for which the individual quark momenta sum up as $\sum \vec{k}_i = 0$. The third line in Eq. (7) expresses the corresponding Lorentz transformation as acting on general three-body states $|p_1, p_2, p_3; \sigma_1, \sigma_2, \sigma_3\rangle$. The quark momenta p_i and k_i are related by $p_i = B(v)k_i$, where $k_i = (\omega_i, \vec{k}_i)$. The $D^{1/2}$ are the spin-$\frac{1}{2}$ representation matrices of Wigner rotations $R_W(k_i, B(v))$. The velocity-state representation allows one to separate the motion of the system as a whole and the internal motion. The latter is described by the wave function $\Psi_{MJ\Sigma}(\vec{k}_i; \mu_i)$, which is also the rest-frame wave function. It contains the whole information on the flavor, spin, and spatial structure of a baryon state.

In the rest frame the invariant mass operator coincides with the Hamiltonian

$$\hat{H} = \hat{H}_{\text{free}} + \hat{H}_{\text{int}} = \hat{H}_{\text{free}} + \sum_{i<j=1}^3 \hat{V}_{ij}, \tag{8}$$

where the quark-quark dynamics is decomposed into a confinement and a hyperfine interaction

$$\hat{H}_{\text{int}} = \sum_{i<j=1}^3 (\hat{V}^{\text{conf}}_{ij} + \hat{V}^{\text{hyper}}_{ij}). \tag{9}$$

While the confinement interaction is nowadays usually taken as a potential linearly rising towards longer distances (as suggested from quantum chromodynamics), the hyperfine interaction is qualitatively distinct among different constituent quark models.

B. Goldstone-boson-exchange RCQM

The Goldstone-boson-exchange (GBE) RCQM [26,27] relies on a linear confinement potential and a hyperfine interaction that is motivated by the spontaneous breaking of chiral symmetry. The different parts in the Hamiltonian are thus represented by

$$H_{\text{free}} = \sum_{i=1}^3 \sqrt{m_i^2 + \vec{k}_i^2}, \tag{10}$$

$$V^{\text{conf}}_{ij} = V_0 + Cr_{ij}, \tag{11}$$

and

$$V^{\text{hf}}_{ij} = \left[\sum_{a=1}^3 V^\pi_{ij}\lambda^a_i\lambda^a_j + \sum_{a=4}^7 V^K_{ij}\lambda^a_i\lambda^a_j + V^\eta_{ij}\lambda^8_i\lambda^8_j + \frac{2}{3}V^{\eta'}_{ij} \right] \vec{\sigma}(i) \cdot \vec{\sigma}(j). \tag{12}$$

The hyperfine interaction is furnished only by the spin-spin part of the GBE (identified with the exchange of pseudo-scalar mesons) and it comes up with an explicit flavor dependence reflected by the $SU(3)$ Gell-Mann flavor matrices λ^a_i in Eq. (12). This specific property is favorable for

a unified description of all light and strange baryon ground and resonance states. In particular, it provides for the correct level orderings of positive- and negative-parity states in both the nucleon and Λ excitation spectra.

The terms V_{ij}^{γ}, with $\gamma = \pi, K, \eta, \eta'$, assume the form of instantaneous meson-exchange potentials. The parameters were determined by fitting the established baryon resonances (with at least three-star status) below 2 GeV. In total, the GBE RCQM involves four open parameters. The detailed parametrization can be found in Ref. [26].

C. One-gluon-exchange RCQM

Another type of RCQM consists in constructing the hyperfine interaction from one-gluon exchange (OGE). Here, we consider, in particular, the relativistic variant of the Bhaduri-Cohler-Nogami OGE CQM [28] in the parametrization of Ref. [9]. The confinement interaction is given by

$$V_{ij}^{\mathrm{conf}} = V_0 + C r_{ij} - \frac{2b}{3r_{ij}}, \qquad (13)$$

and the hyperfine potential relies on the (flavor-independent) color-magnetic spin-spin interaction

$$V_{ij}^{\mathrm{hf}} = \frac{\alpha_S}{9m_i m_j} \Lambda^2 \frac{e^{-\Lambda r_{ij}}}{r_{ij}} \vec{\sigma}(i) \cdot \vec{\sigma}(j). \qquad (14)$$

The OGE RCQM also has four open parameters that were obtained through a fit to the baryon spectrum. The detailed parametrization is given in Ref. [9].

III. BARYON SPECTRA

The solution of the eigenvalue problem of the mass operator $\hat{M}$ in Eq. (2) has been performed with the stochastic variational method (SVM) [29]. Thereby we have produced the invariant mass spectra of all the light and strange baryons [30]. In addition we have obtained the rest-frame wave functions of all ground and resonance states.

The energy eigenvalues of the ground states and resonances below ≈ 2 GeV as resulting with the GBE and OGE RCQMs are quoted in Table I. Here, only eigenstates with (rest-frame) total orbital angular momentum $L < 2$ are considered, as the theoretical decay properties necessary in the present work are available only for such states [1–3]. For the complete spectra of the GBE and OGE RCQMs we refer to Refs. [9,26,27], respectively. The same results are depicted also in Figs. 1 and 2 in comparison to the phenomenological data by the Particle Data Group (PDG) [15]. The left (red) lines in each one of the J^P columns denote the energy levels produced by the OGE RCQM, while the right (red) lines belong to the GBE RCQM. With respect to the number of states below about 2 GeV one immediately observes a one-to-one correspondence between theory and experiment in each one of the J^P

sets in the light-flavor sector (Fig. 1). In the strange sector (Fig. 2), however, there would be more theoretical levels than experimental ones, if only established resonances

TABLE I. Energy eigenvalues (in MeV) of the ground and resonance states with total angular momentum and parity J^P from the GBE and OGE RCQMs in comparison to the experimental masses according to the PDG [15]. In each case the number in the parentheses denotes the kth excitation in the respective J^P column starting with $k = 0$. The resonances denoted by mass values in square brackets represent states not definitely classified by the PDG.

| Baryon	J^P	Theory		Experiment
		GBE	OGE	
$N(939)$	$\frac{1}{2}^+$	939 (0)	939 (0)	938–940
$N(1440)$	$\frac{1}{2}^+$	1459 (1)	1577 (1)	1420–1470
$N(1520)$	$\frac{3}{2}^-$	1519 (0)	1521 (0)	1515–1525
$N(1535)$	$\frac{1}{2}^-$	1519 (0)	1521 (0)	1525–1545
$N(1650)$	$\frac{1}{2}^-$	1647 (1)	1690 (1)	1645–1670
$N(1675)$	$\frac{5}{2}^-$	1647 (0)	1690 (0)	1670–1680
$N(1700)$	$\frac{3}{2}^-$	1647 (1)	1690 (1)	1650–1750
$N(1710)$	$\frac{1}{2}^+$	1776 (2)	1859 (2)	1680–1740
$\Delta(1232)$	$\frac{3}{2}^+$	1240 (0)	1231 (0)	1231–1233
$\Delta(1600)$	$\frac{3}{2}^+$	1718 (1)	1854 (1)	1550–1700
$\Delta(1620)$	$\frac{1}{2}^-$	1642 (0)	1621 (0)	1600–1660
$\Delta(1700)$	$\frac{3}{2}^-$	1642 (0)	1621 (0)	1670–1750
$\Lambda(1116)$	$\frac{1}{2}^+$	1136 (0)	1113 (0)	1116
$\Lambda(1405)$	$\frac{1}{2}^-$	1556 (0)	1628 (0)	1402–1410
$\Lambda(1520)$	$\frac{3}{2}^-$	1556 (0)	1628 (0)	1519–1521
$\Lambda(1600)$	$\frac{1}{2}^+$	1625 (1)	1747 (1)	1560–1700
$\Lambda(1670)$	$\frac{1}{2}^-$	1682 (1)	1734 (1)	1660–1680
$\Lambda(1690)$	$\frac{3}{2}^-$	1682 (1)	1734 (1)	1685–1695
$\Lambda(1800)$	$\frac{1}{2}^-$	1778 (2)	1844 (2)	1720–1850
$\Lambda(1810)$	$\frac{1}{2}^+$	1799 (2)	1957 (2)	1750–1850
$\Lambda(1830)$	$\frac{5}{2}^-$	1778 (0)	1844 (0)	1810–1830
$\Sigma(1193)$	$\frac{1}{2}^+$	1180 (0)	1213 (0)	1189–1197
$\Sigma(1385)$	$\frac{3}{2}^+$	1389 (0)	1373 (0)	1383–1387
$\Sigma[1560]$	$\frac{1}{2}^-$	1677 (0)	1732 (0)	1546–1576
$\Sigma[1620]$	$\frac{1}{2}^-$	1736 (1)	1829 (2)	1594–1643
$\Sigma(1660)$	$\frac{1}{2}^+$	1616 (1)	1845 (1)	1630–1690
$\Sigma(1670)$	$\frac{3}{2}^-$	1677 (0)	1732 (0)	1665–1685
$\Sigma[1690]$	$\frac{3}{2}^+$	1865 (1)	1991 (1)	1670–1727
$\Sigma(1750)$	$\frac{1}{2}^-$	1759 (2)	1784 (1)	1730–1800
$\Sigma(1775)$	$\frac{5}{2}^-$	1736 (0)	1829 (0)	1770–1780
$\Sigma(1880)$	$\frac{1}{2}^+$	1911 (2)	2049 (2)	1806–2025
$\Sigma[1940]$	$\frac{3}{2}^-$	1736 (1)	1829 (2)	1900–1950
Σ	$\frac{3}{2}^-$	1759 (2)	1784 (1)	
$\Xi(1318)$	$\frac{1}{2}^+$	1348 (0)	1346 (0)	1315–1321
$\Xi(1530)$	$\frac{3}{2}^+$	1528 (0)	1516 (0)	1532–1535
$\Xi[1690]$	$\frac{1}{2}^+$	1805 (1)	1975 (1)	1680–1700
$\Xi(1820)$	$\frac{3}{2}^-$	1792 (0)	1894 (0)	1818–1828
$\Xi[1950]$	$\frac{5}{2}^-$	1881 (0)	1993 (0)	1935–1965
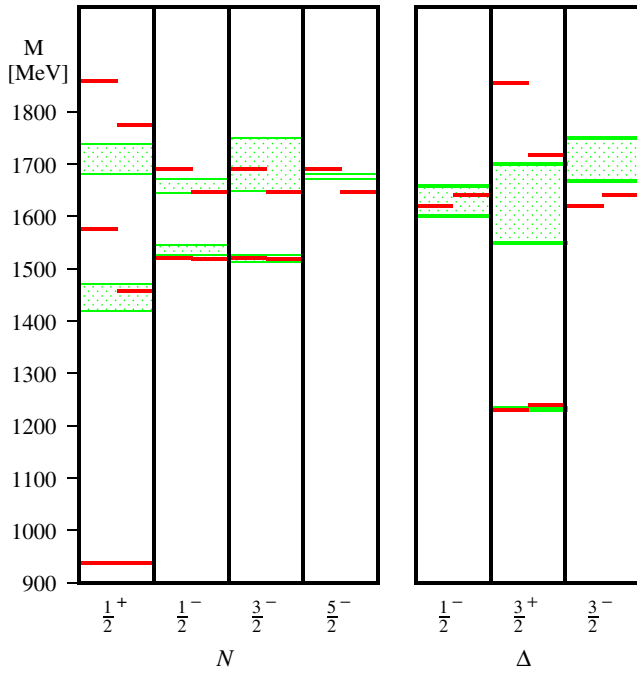
FIG. 1 (color online). Energy levels (solid red lines) of the lowest N and Δ states with total angular momentum and parity J^P for the OGE (left levels) and GBE (right levels) RCQMs in comparison to experimental values with uncertainties [15], represented as shadowed (green) boxes.

(with at least three-star status) were taken into account. For instance, in the $J^P = \frac{1}{2}^-$ column of the Σ excitation spectrum the RCQMs produce three states, while there is only

one established resonance reported. This problem is remedied, if one includes also the two lower-lying resonances $\Sigma(1560)$ and $\Sigma(1620)$, as is done in Fig. 2. Of course, these two resonances have only a two-star confidence status and the J^P value is only known for the latter [32]. As will become clear in the subsequent sections, these additional states are required and can/should be accommodated in a consistent classification into $SU(3)$ flavor multiplets. A similar situation occurs in the $J^P = \frac{3}{2}^-$ Σ spectrum, where the RCQMs again produce three levels, while the PDG reports only two established resonances. In this case, however, there is essentially no further candidate seen in experiment, even not with one- or two-star status. Therefore the RCQM state that misses a corresponding experimental counterpart (the last Σ entry in Table I) is indicated by dashed lines in Fig. 2. Nevertheless, all of these three theoretical states fit into the $SU(3)$ multiplet classification we propose in the following sections.

The PDG [15] gives assignments of baryon states (for $L < 2$) in terms of flavor multiplets as summarized in Table II. In this context not only established (three- and four-star) resonances are included but also some two-star states. Besides the octet and decuplet of ground states only one more multiplet is complete, namely, the octet of the lowest $J^P = \frac{3}{2}^-$ excitations [involving the $N(1520)$ resonance]. All other multiplets miss at least a Ξ, the decuplets in addition also a Σ. The assignments of some states, especially of $\Lambda(1810)$ and $\Xi(1820)$, are merely based on educated guesses [15]. The resulting scheme is mostly in line with the one by Samios, Goldberg, and Meadows
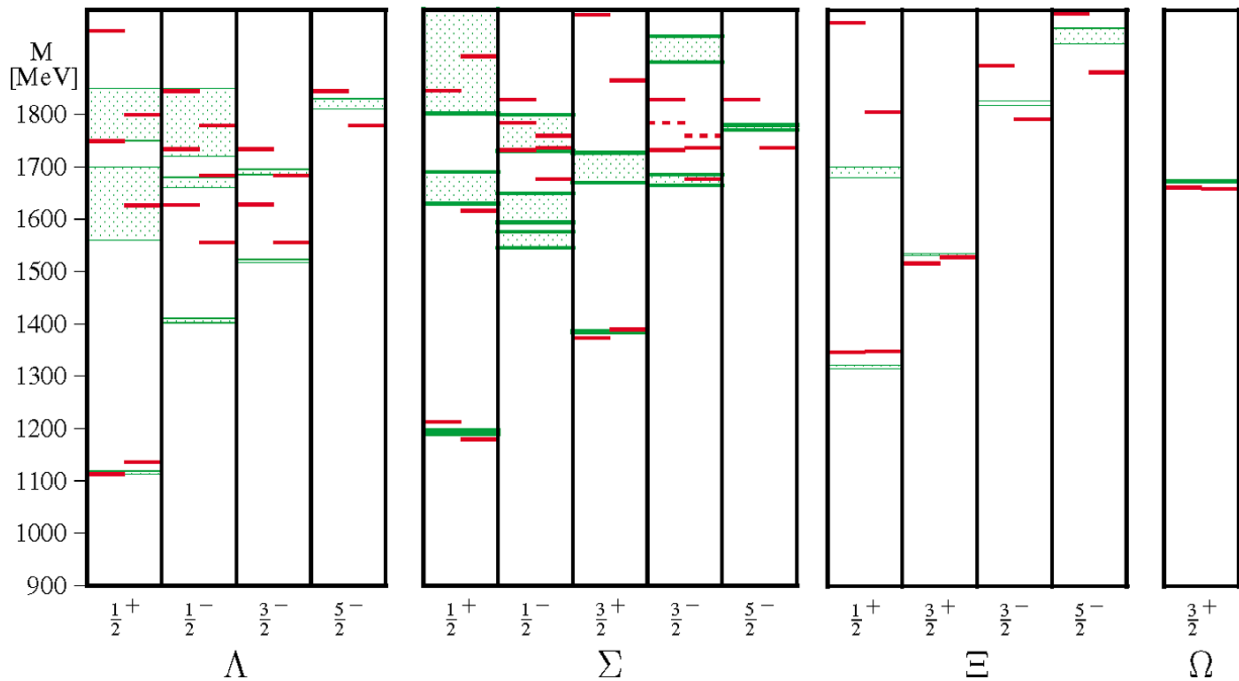

FIG. 2 (color online). Same as in Fig. 1 for the lowest Λ, Σ, Ξ, and Ω states. The dashed lines in the $J^P = \frac{3}{2}^-$ Σ spectrum represent (decuplet) eigenstates, for which there is no experimental counterpart yet.

TABLE II. Classification of baryon ground and resonance states into flavor multiplets by the PDG [15]. In addition to established states also some two-star resonances are included, namely, $\Sigma(1620)$ and $\Sigma(1880)$. Entries with question marks have not yet received any assignments.

Multiplet	$(LS)J^P$			
Octet	$(0\frac{1}{2})\frac{1}{2}^+$	$N(939)$	$\Lambda(1116)$	$\Sigma(1193)$	$\Xi(1318)$
Octet	$(0\frac{1}{2})\frac{1}{2}^+$	$N(1440)$	$\Lambda(1600)$	$\Sigma(1660)$	$\Xi(?)$
Octet	$(0\frac{1}{2})\frac{1}{2}^+$	$N(1710)$	$\Lambda(1810)$	$\Sigma(1880)$	$\Xi(?)$
Octet	$(1\frac{1}{2})\frac{1}{2}^-$	$N(1535)$	$\Lambda(1670)$	$\Sigma(1620)$	$\Xi(?)$
Octet	$(1\frac{3}{2})\frac{1}{2}^-$	$N(1650)$	$\Lambda(1800)$	$\Sigma(1750)$	$\Xi(?)$
Octet	$(1\frac{1}{2})\frac{3}{2}^-$	$N(1520)$	$\Lambda(1690)$	$\Sigma(1670)$	$\Xi(1820)$
Octet	$(1\frac{3}{2})\frac{3}{2}^-$	$N(1700)$	$\Lambda(?)$	$\Sigma(?)$	$\Xi(?)$
Octet	$(1\frac{3}{2})\frac{5}{2}^-$	$N(1675)$	$\Lambda(1830)$	$\Sigma(1775)$	$\Xi(?)$
Singlet	$(1\frac{1}{2})\frac{1}{2}^-$	$\cdots$	$\Lambda(1405)$	$\cdots$	$\cdots$
Singlet	$(1\frac{1}{2})\frac{3}{2}^-$	$\cdots$	$\Lambda(1520)$	$\cdots$	$\cdots$
Decuplet	$(0\frac{3}{2})\frac{3}{2}^+$	$\Delta(1232)$	$\cdots$	$\Sigma(1385)$	$\Xi(1530)$
Decuplet	$(0\frac{3}{2})\frac{3}{2}^+$	$\Delta(1600)$	$\cdots$	$\Sigma(?)$	$\Xi(?)$
Decuplet	$(1\frac{1}{2})\frac{1}{2}^-$	$\Delta(1620)$	$\cdots$	$\Sigma(?)$	$\Xi(?)$
Decuplet	$(1\frac{1}{2})\frac{3}{2}^-$	$\Delta(1700)$	$\cdots$	$\Sigma(?)$	$\Xi(?)$

[33] proposed back in 1974, when many of the resonances known today have not yet been found from phenomenology.

To a large extent the PDG classification also coincides with a more recent one by Guzey and Polyakov (GP) [34]. There occur only differences with regard to the identification of the $\Sigma(1620)$ in the $J^P = \frac{1}{2}^-$ octet, involving the $N(1535)$, and the $\Sigma(1750)$ in the $J^P = \frac{1}{2}^-$ octet, involving the $N(1650)$; according to GP the $\Sigma(1750)$ falls into the $J^P = \frac{1}{2}^-$ decuplet involving the $\Delta(1620)$. In addition, some further states without assignment by the PDG were included by GP, such as the three-star resonances $\Xi(1690)$ and $\Xi(1950)$ as well as the two-star resonances $\Sigma(1560)$ and $\Sigma(1690)$. All of the latter will also be considered (and needed) in the classification we elaborate and propose below.

IV. MESONIC DECAYS OF ESTABLISHED BARYON RESONANCES

The mesonic decays of the baryon resonances from Figs. 1 and 2 were comprehensively studied with regard to their π, η, and K decay modes within a relativistic framework [1–3]. In these works the decay operator was constructed along the point-form spectator model (PFSM) [35]. It consists in the simplifying assumption that the meson is emitted from one quark while the other two act as spectators. The PFSM decay operator is manifestly covariant and it preserves its spectator-model character in all reference frames. Though it formally looks like a one-body operator, it nevertheless includes many-body effects [20]. In particular, the recoil effect on the residual baryon

state is naturally taken into account. The nonrelativistic limit of the PFSM leads to the familiar elementary emission model (EEM).

From the covariant PFSM calculations a new pattern of partial decay widths as predicted by modern RCQMs has emerged. It has turned out to be rather different from what had been known from previous nonrelativistic or relativized studies. Notably, quite large relativistic effects have been detected, and the results generally underestimate the experimental data. In this context it is remarkable that quite similar findings have been obtained by the Bonn group from a completely different relativistic investigation along the Bethe-Salpeter formalism [10,11].

In Fig. 3 the situation is exemplified with regard to the low-lying octet baryon resonances for which partial decay widths are reported by the PDG. The theoretical decay widths as resulting with the GBE RCQM are depicted as percentages of the (best estimates of the) experimental data. In each octet one observes a clear pattern: The magnitudes of the theoretical widths remain far below the experimental measurements, i.e. they lie to the left of the vertical 100% lines. There are only a few exceptions. In the octet involving the $N(1710)$ the decay width for the $N\pi$ mode appears to be unusually large. The same is true for the $\Lambda \rightarrow \Sigma\pi$ decays in the $N(1535)$ and $N(1520)$ octets. Regarding the η decays the relatively large percentages should not be taken too seriously in the cases of $N(1700)$ and $N(1675)$ as the magnitudes of the experimental widths are very small, practically identical to zero. In the η channel only two partial widths are sizable, namely, the ones of $N(1535)$ and $N(1650)$. The latter one comes out considerably larger than experimentally measured. This must be considered as a notorious problem of constituent quark models and may point to an unidentified deficiency in the decay operator and/or resonance wave function.

Of particular interest in the context of the present study are the π decays of the $J^P = \frac{1}{2}^-$ Σ resonances. Out of the three eigenstates appearing in Fig. 2 two of them are octets, as can be clearly determined from the RCQM calculations. If one considers only resonances with at least three-star status and known phenomenological partial decay widths, these two octet states should be related to the $\Sigma(1750)$ resonance. In Fig. 3 their $\Sigma \rightarrow \Sigma\pi$ decay widths are represented relative to the experimental width measured for $\Sigma(1750)$. They are denoted by the double triangles, since for both octet states when interpreted in this manner the theoretical results grossly overshoot the data. However, we must consider that there are two further Σ resonances observed in experiments that may be taken as candidates for the identification of the $J^P = \frac{1}{2}^-$ eigenstates, namely, the unassigned $\Sigma(1560)$ and the $J^P = \frac{1}{2}^-$ $\Sigma(1620)$, both with two-star status. If the $J^P = \frac{1}{2}^-$ Σ octet states are related to these resonances, then the third eigenstate, found to be a decuplet state in the RCQM calculations, has to be interpreted as $\Sigma(1750)$. In this way the decay widths of all
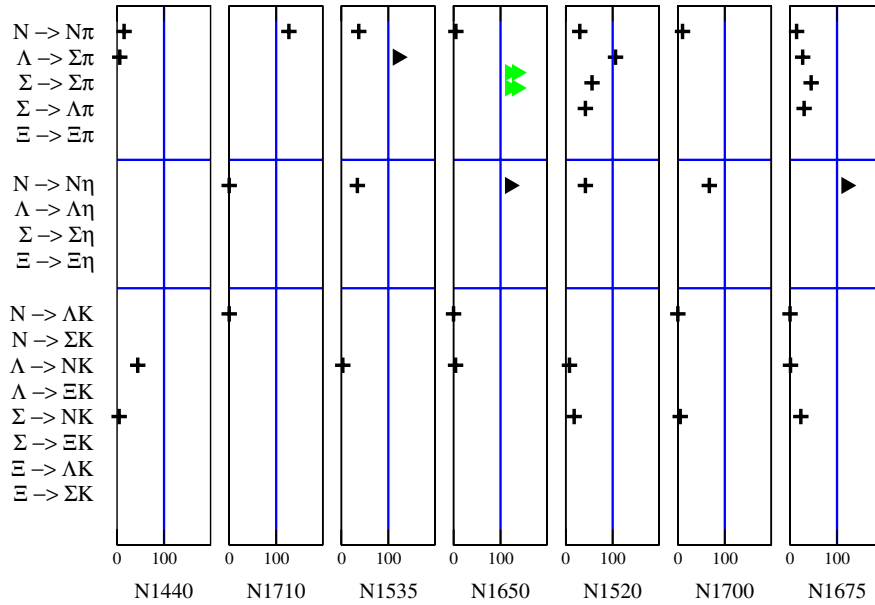
FIG. 3 (color online).   Predictions for partial π, η, and K decay widths of the GBE CQM from the PFSM calculation for the lowest octets according to Refs. [1–3]. The results (crosses) are presented as percentages of the best estimates for experimental data reported by the PDG [15]. The various resonances are grouped according to the octet assignments in Table II. The (double) triangles point to results (far) outside the plotted range. For the latter see also the discussion in the text.

three $J^P = \frac{1}{2}^-$ Σ fit into the general pattern of relativistic mesonic decay widths [2] (cf. the results presented in Sec. VI below).

One may ask for the causes of the deficiencies of the relativistic spectator-model calculations, especially also in view of results existing in the literature with apparently better agreement with phenomenology. Past studies have revealed that a nonrelativistic spectator-model decay operator, such as the EEM, is not sufficiently sophisticated to yield a reasonable description of the mesonic decays. A more elaborate decay mechanism is provided, for example, by the relativized pair-creation model [36]. Studies along this line were performed among others in Refs. [4–6,9]. All of these works have in common that some additional parametrizations were introduced on top of the direct predictions of the underlying constituent quark models. In this way one adjusted the extensions of the meson-creation vertices and/or the coupling strengths. Furthermore, different phase-space factors were employed in the decay amplitude. As a result the different approaches can hardly be compared to each other and the degree of agreement with experimental data does not really allow one to judge on the appropriateness of the approach followed. So, it could well be that missing relativistic effects or other shortcomings either of the quark-model wave functions or the decay operator were compensated by introducing *ad hoc* parameters.

For the relativistic results of decay widths reported in Refs. [1–3] as well as in Refs. [10,11] one refrained from applying any additional parametrization to the predictions

of the RCQMs. Even though in these works by the Bonn and Graz groups different RCQMs were employed and distinct relativistic approaches were followed, the predicted decay widths came out surprisingly similar. This might be a consequence of implementing full Poincaré invariance, which is strictly observed in our point-form approach and similarly in the Bethe-Salpeter formalism followed by the Bonn group. In both types of relativistic studies one lacks substantial contributions to the mesonic decay widths. One is left with a systematic underestimation of the experimental data with only a few exceptional cases. In view of the present insight it is difficult to decide from where the defects come. However, one must bear in mind that in present-day constituent quark models the baryon ground and resonance states are all described as bound three-quark eigenstates of the invariant mass operator. In addition, the decay operators used so far might miss important contributions from explicit many-body parts. Still, the covariant results achieved so far can serve as benchmarks and provide a solid basis for further explorations.

In the following section we present a classification of the singlet, octet, and decuplet baryon resonances based on the evidence of their properties from the mass spectra, the mesonic decay widths as well as the spin-flavor contents and the spatial structures of the wave functions. It will turn out that for a comprehensive classification of the various states we shall need to consider the decay widths of additional RCQM eigenstates beyond the results already published in Refs. [1–3]. The corresponding predictions are collected in Table III.

TABLE III. Covariant predictions of partial widths for various decay modes of hyperon resonances by the GBE CQM [26] and the OGE CQM [9]. The denotation of the states follows the multiplet assignments in the present work (see Tables IV, V, and VI). Regarding phenomenological data [15] a comparison is possible only to total decay widths.

Decay	J^P	Experiment [MeV]	With theoretical masses		With experimental masses	
			GBE	OGE	GBE	OGE
$\rightarrow \Sigma\pi$						
$\Sigma(1560)$	$\frac{1}{2}^-$	$\Gamma(9{-}109)$	58	102	44	70
$\Sigma(1620)$	$\frac{1}{2}^-$	$\Gamma(10{-}106)$	32	44	21	26
$\Sigma(1690)$	$\frac{3}{2}^+$	$\Gamma(15{-}300)$	0.4	2.7	0.2	1.1
$\Sigma(1880)$	$\frac{1}{2}^+$	$\Gamma(30{-}372)$	3.0	3.0	1.8	0.4
$\rightarrow \Lambda\pi$						
$\Sigma(1560)$	$\frac{1}{2}^-$	$\Gamma(9{-}109)$	1.6	1.5	2.1	2.2
$\Sigma(1620)$	$\frac{1}{2}^-$	$\Gamma(10{-}106)$	19	25	17	23
$\Sigma(1690)$	$\frac{3}{2}^+$	$\Gamma(15{-}300)$	≈ 0	1.2	≈ 0	0.6
$\Sigma(1880)$	$\frac{1}{2}^+$	$\Gamma(30{-}372)$	1.7	0.5	1.6	0.3
$\rightarrow NK$						
$\Sigma(1560)$	$\frac{1}{2}^-$	$\Gamma(9{-}109)$	8	8	6	5
$\Sigma(1620)$	$\frac{1}{2}^-$	$\Gamma(10{-}106)$	55	55	57	58
$\Sigma(1690)$	$\frac{3}{2}^+$	$\Gamma(15{-}300)$	≈ 0	1.4	≈ 0	0.8
$\Sigma(1880)$	$\frac{1}{2}^+$	$\Gamma(30{-}372)$	≈ 0	≈ 0	≈ 0	≈ 0
$\rightarrow \Xi\pi$						
$\Xi(1690)$	$\frac{1}{2}^+$	$\Gamma(<30)$	0.8	1.8	0.5	0.5
$\Xi(1950)$	$\frac{5}{2}^-$	$\Gamma(40{-}80)$	14	28	25	26
$\rightarrow \Lambda K$						
$\Xi(1690)$	$\frac{1}{2}^+$	$\Gamma(<30)$	1.1	1.3	0.5	0.4
$\Xi(1950)$	$\frac{5}{2}^-$	$\Gamma(40{-}80)$	2.5	4.4	4.3	3.6
$\rightarrow \Sigma K$						
$\Xi(1690)$	$\frac{1}{2}^+$	$\Gamma(<30)$	9.2	55	0.1	0.2
$\Xi(1950)$	$\frac{5}{2}^-$	$\Gamma(40{-}80)$	2.3	4.3	3.7	3.6
$\rightarrow \Xi\eta$						
$\Xi(1950)$	$\frac{5}{2}^-$	$\Gamma(40{-}80)$		≈ 0	0.1	0.1

V. CLASSIFICATION OF BARYON RESONANCES

In order to arrive at a conclusive assignment of RCQM eigenstates to $SU(3)$ multiplets we now analyze the spin-flavor contents and spatial structures of the baryon wave functions. Through the results from the solution of the mass-operator eigenvalue problem with the SVM we have access to their detailed dependences on flavor, spin, and spatial variables. The SVM uses a completely general basis of flavor, spin, and spatial test functions. In the process of stochastic variation they are selected by varying all flavor, spin, orbital angular momentum, and radial dependences so as to couple to baryon states characterized by definite intrinsic spin J, z component Σ, hypercharge Y, total isospin T as well as isospin z component M_T (for details see Ref. [37]). In practice the eigenvalue problem is solved in the rest frame of the corresponding state, where the point-form version of relativistic quantum mechanics is employed. We note, however, that the solution for the mass spectra is relativistically invariant and thus independent of the specific form of relativistic quantum mechanics.

A. Spin-flavor content of baryons

In our solution of the mass-operator eigenvalue problem (in the rest frame) utilizing the SVM, the total orbital angular momentum is restricted to $L < 2$. Even higher angular-momentum components have turned out to be rather small and may be neglected for the ground and resonance states considered here. For any eigenstate the total spin S is definitely determined. L and S uniquely produce the intrinsic spin J and parity P.

With regard to the flavor content, the SVM may pick up basis states from different $SU(3)$ flavor multiplets. In particular, mixtures of flavor contributions from singlet and octet as well as octet and decuplet can occur. This happens specifically for the Λ, Σ, and Ξ hyperons. For their mass-operator eigenstates we can easily determine the singlet, octet, and decuplet contents, respectively. For this purpose

we employ the appropriate flavor projection operators. For the singlet it reads

$$P_1^F = \tfrac{1}{6}(|uds\rangle - |usd\rangle + |dsu\rangle - |dus\rangle + |sud\rangle - |sdu\rangle)$$
$$\times (\langle uds| - \langle usd| + \langle dsu| - \langle dus| + \langle sud| - \langle sdu|).$$

Evidently it sorts out the completely antisymmetric singlet component of a certain baryon state whose probability is then given by

$$\alpha^1 = \langle V, J, M, \Sigma | P_F^1 | V, J, M, \Sigma \rangle. \tag{15}$$

For the special case of singlet-octet mixing, such as Λ, the octet probability is then simply

$$\alpha^8 = 1 - \alpha^1. \tag{16}$$

Similarly, for the Σ and Ξ baryons, mixtures between flavor octet and decuplet can occur. Here, we determine the decuplet content by employing the decuplet projection operator P_F^{10}. In the case of Σ it suffices to consider the corresponding projection operator for Σ^0

$$P_F^{10}(\Sigma^0) = \tfrac{1}{6}(|uds\rangle + |usd\rangle + |dsu\rangle + |dus\rangle + |sud\rangle$$
$$+ |sdu\rangle)(\langle uds| + \langle usd| + \langle dsu|$$
$$+ \langle dus| + \langle sud| + \langle sdu|),$$

since the decuplet content is the same for Σ^+ and Σ^- due to isospin symmetry. Analogous considerations hold for the Ξ states, and we may use the decuplet projection operator

$$P_F^{10}(\Xi^0) = \tfrac{1}{3}(|ssu\rangle + |sus\rangle + |uss\rangle)(\langle ssu| + \langle sus|$$
$$+ \langle uss|).$$

Again, the octet content is obtained by

$$\alpha^8 = 1 - \alpha^{10}. \tag{17}$$

B. Spatial structure of baryons

For the characterization of the spatial structure of any baryon ground state or resonance we consider the angle-integrated spatial probability density distribution

$$\rho(\xi, \eta) = \xi^2 \eta^2 \int d\Omega_\xi d\Omega_\eta \Psi^*_{M\Sigma M_\Sigma T M_T}(\xi, \Omega_\xi, \eta, \Omega_\eta)$$
$$\times \Psi_{M\Sigma M_\Sigma T M_T}(\xi, \Omega_\xi, \eta, \Omega_\eta), \tag{18}$$

where $\vec{\xi} = (\xi, \Omega_\xi)$ and $\vec{\eta} = (\eta, \Omega_\eta)$ are the Jacobi coordinates. It provides an idea of the matter distribution in a baryon. In Fig. 4 probability density distributions are exemplified for the nucleon ground state and the Roper resonance. Whereas the nucleon shows a rather symmetric shape with the density distribution peaked at a root-mean-square radius of about 0.3 fm, the $N(1440)$ exhibits the typical behavior of a first radial excitation, i.e. with a nodal line in the wave function. One also observes that $\rho(\xi, \eta)$ is

N GBE CQM   N OGE CQM

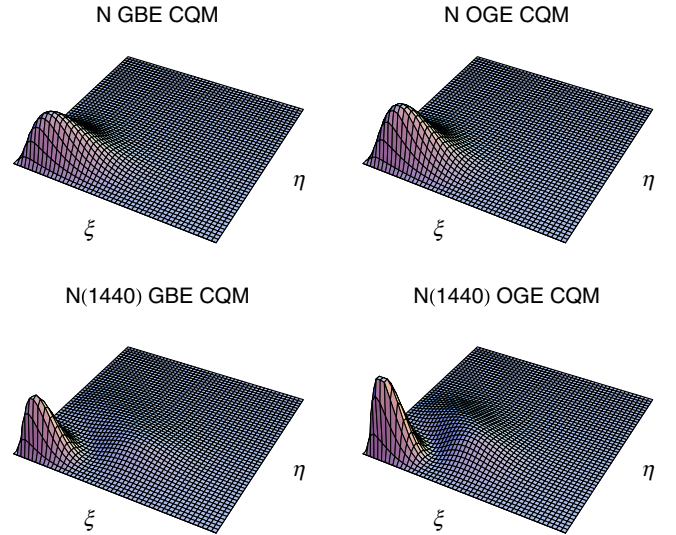N(1440) GBE CQM   N(1440) OGE CQM

FIG. 4 (color online). Spatial probability density distributions $\rho(\xi, \eta)$ of the nucleon ground state $N(939)$ and the Roper resonance $N(1440)$ as a function of the radial parts of the Jacobi coordinates ξ and η for the GBE RCQM (left plots) and the OGE RCQM (right plots).

very similar for both the GBE and OGE RCQMs. The latter is slightly more localized, as its confinement interaction is relatively stronger. In the following subsections we therefore restrict ourselves to showing only the probability density distributions for the GBE RCQM.

C. Baryon multiplets

For the relativistic mass-operator eigenstates we obtain the flavor-multiplet classifications as given in Tables IV, V, and VI. We group the states according to their (LS) values which determine the J^P. Evidently not all states have a pure singlet, octet, or decuplet content. In particular, considerable admixtures can occur for the Λ singlet and octet states.

1. Octet: $N(939)$, $\Lambda(1116)$, $\Sigma(1193)$, $\Xi(1318)$

The identification of the octet ground states is natural, all bear total intrinsic spin and parity $J^P = \tfrac{1}{2}^+$, and they have pure octet flavor content. The corresponding spatial probability densities are plotted in Fig. 5. They all exhibit the typical behavior of ground states with no nodal lines. It should be noted that with these eigenstates all electroweak properties of the nucleons as well as the electric radii and magnetic moments of the other ground states are predicted in good agreement with experiment [17–21].

2. Decuplet: $\Delta(1232)$, $\Sigma(1385)$, $\Xi(1530)$, $\Omega(1672)$

The classification of the lowest decuplet states $\Delta(1232)$, $\Sigma(1385)$, $\Xi(1530)$, and $\Omega(1672)$ is also straightforward. All are characterized by $J^P = \tfrac{3}{2}^+$, where $L = 0$ and $S = \tfrac{3}{2}$. The eigenstates are totally symmetric with respect to spin

TABLE IV. Classification of flavor octet baryons. The denotation of the mass eigenstates is made according to the nomenclature of baryon states seen in experiment. The superscripts denote the percentages of octet content as calculated with the GBE CQM [26]. States in boldface either have not been assigned by the PDG or differ from their assignment.

$(LS)J^P$				
$(0\frac{1}{2})\frac{1}{2}^+$	$N(939)^{100}$	$\Lambda(1116)^{100}$	$\Sigma(1193)^{100}$	$\Xi(1318)^{100}$
$(0\frac{1}{2})\frac{1}{2}^+$	$N(1440)^{100}$	$\Lambda(1600)^{96}$	$\Sigma(1660)^{100}$	$\Xi(\mathbf{1690})^{100}$
$(0\frac{1}{2})\frac{1}{2}^+$	$N(1710)^{100}$		$\Sigma(1880)^{99}$	
$(1\frac{1}{2})\frac{1}{2}^-$	$N(1535)^{100}$	$\Lambda(1670)^{72}$	$\mathbf{\Sigma(1560)}^{94}$	
$(1\frac{3}{2})\frac{1}{2}^-$	$N(1650)^{100}$	$\Lambda(1800)^{100}$	$\mathbf{\Sigma(1620)}^{100}$	
$(1\frac{1}{2})\frac{3}{2}^-$	$N(1520)^{100}$	$\Lambda(1690)^{72}$	$\Sigma(1670)^{94}$	$\Xi(1820)^{97}$
$(1\frac{3}{2})\frac{3}{2}^-$	$N(1700)^{100}$		$\mathbf{\Sigma(1940)}^{100}$	
$(1\frac{3}{2})\frac{5}{2}^-$	$N(1675)^{100}$	$\Lambda(1830)^{100}$	$\Sigma(1775)^{100}$	$\mathbf{\Sigma(1950)}^{100}$

TABLE V. Classification of flavor decuplet baryons. Analogous notation as in Table IV.

$(LS)J^P$				
$(0\frac{3}{2})\frac{3}{2}^+$	$\Delta(1232)^{100}$	$\Sigma(1385)^{100}$	$\Xi(1530)^{100}$	$\Omega(1672)^{100}$
$(0\frac{3}{2})\frac{3}{2}^+$	$\Delta(1600)^{100}$	$\mathbf{\Sigma(1690)}^{99}$		
$(1\frac{1}{2})\frac{1}{2}^-$	$\Delta(1620)^{100}$	$\mathbf{\Sigma(1750)}^{94}$		
$(1\frac{1}{2})\frac{3}{2}^-$	$\Delta(1700)^{100}$			

TABLE VI. Classification of flavor singlet baryons. Analogous notation as in Table IV.

$(LS)J^P$	
$(1\frac{1}{2})\frac{1}{2}^-$	$\Lambda(1405)^{71}$
$(1\frac{1}{2})\frac{3}{2}^-$	$\Lambda(1520)^{71}$
$(0\frac{1}{2})\frac{1}{2}^+$	$\mathbf{\Lambda(1810)}^{92}$

and flavor. This leads to similar spatial probability densities as for the octet ground states but with a larger extension (see Fig. 6).

3. Octet: $N(1440)$, $\Lambda(1600)$, $\Sigma(1660)$, $\Xi(1690)$

The states $N(1440)$, $\Lambda(1600)$, $\Sigma(1660)$, and $\Xi(1690)$ represent the first radial excitations with $J^P = \frac{1}{2}^+$ above the octet ground states. Their spatial probability densities are shown in Fig. 7, with all of them exhibiting the typical nodal structures. The RCQM predicts all of these states to be pure flavor octets with the exception of the $\Lambda(1600)$, which has a singlet contribution of 4%. For the Ξ member of this multiplet the GBE RCQM produces an eigenstate with a theoretical mass of 1805 MeV. We may identify it with the $\Xi(1690)$ resonance, which appears as a three-star resonance with no J^P value in the listings of the PDG and is not included in their multiplet assignments (cf. Table II).

Similarly, GP classify the $\Xi(1690)$ into the $J^P = \frac{1}{2}^+$ octet [34]. The $\Xi(1690)$ is tentatively a spin-$\frac{1}{2}$ state [38]. As we shall see in the next section, the decay width of the theoretical $J^P = \frac{1}{2}^+$ Ξ state at least fits into the general pattern observed for the PFSM results and the magnitude of the total width is in line with the value measured by the *BABAR* Collaboration [38]. On the other hand, in a recent study Pervin and Roberts [39] classify the $\Xi(1690)$ as a $J^P = \frac{1}{2}^-$ octet resonance. More conclusive experimental data on this state would be highly welcome in order to clarify the situation with respect to its parity.

4. Octet: $N(1710)$, $\Sigma(1880)$

For the second octet of excited states with $J^P = \frac{1}{2}^+$ we can only classify the $N(1710)$ and the $\Sigma(1880)$. They both have $L = 0$ and $S = \frac{1}{2}$ and are predominantly of mixed flavor-spin symmetry. These resonances are characterized by the typical spatial probability density distributions of second radial excitations as shown in Fig. 8, with a dip following a straight line through the origin of the (ξ, η) plane. The flavor content of these two resonances is practically pure octet. The $\Sigma(1880)$ resonance has only two-star status, while its J^P is experimentally confirmed to be $\frac{1}{2}^+$. Besides the $\Sigma(1620)$ it is the only two-star resonance that is taken into account by the PDG, and they classify it into the same octet as we do.

The PDG classifies also the $\Lambda(1810)$ to be a member of this octet. However, in the RCQMs no flavor octet Λ state with $J^P = \frac{1}{2}^+$ is found below 2 GeV; rather one obtains a flavor singlet. Thus the classification of the Λ and likewise the Ξ members of this octet must be left open, as the possible candidates $\Lambda(2000)$ and $\Xi(2120)$, or even higher Ξ's, are not well enough established experimentally.

5. Singlet: $\Lambda(1810)$

The RCQMs produce a $J^P = \frac{1}{2}^+$ with $L = 0$ and $S = \frac{1}{2}$ at an energy of 1799 and 1957 MeV for the GBE and OGE hyperfine interactions, respectively. They are definitely flavor singlets with only a few percent of octet admixture. No other suitable Λ resonances are found below 2 GeV. Therefore we identify this $J^P = \frac{1}{2}^+$ eigenstate with the $\Lambda(1810)$. While this classification differs from the one by the PDG, the same identification as ours is also suggested by Matagne and Stancu [40]. The probability density distribution of the $\Lambda(1810)$ is depicted in Fig. 9.

6. Singlet: $\Lambda(1405)$

The state $\Lambda(1405)$ is predominantly a flavor singlet with $J^P = \frac{1}{2}^-$, and it is constructed from $L = 1$ and $S = \frac{1}{2}$. The octet admixture is about one-third, by far larger as in the case of $\Lambda(1810)$. The corresponding probability density distribution is also shown in Fig. 9. It should be mentioned that the $\Lambda(1405)$ represents a notorious difficulty in reproducing its mass for all constituent quark models relying on
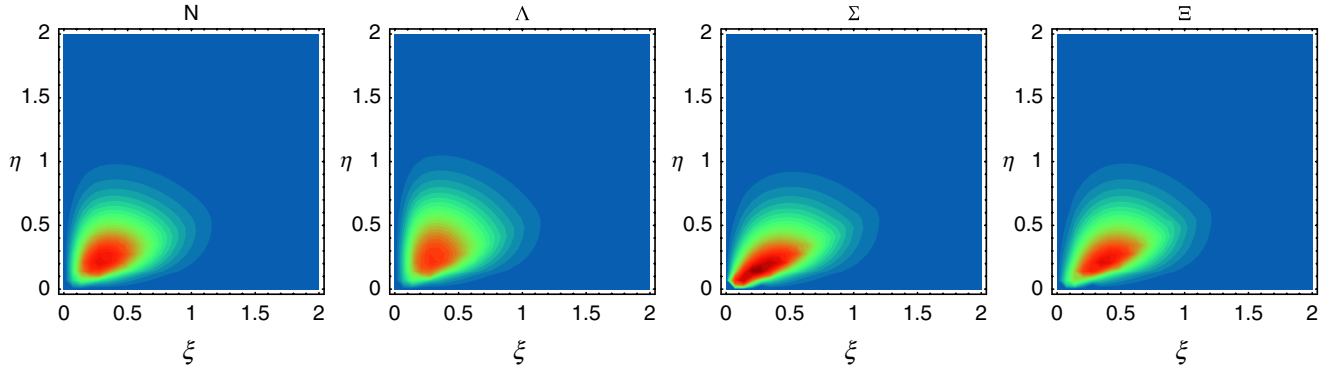
FIG. 5 (color online). Spatial probability density distributions $\rho(\xi, \eta)$ of the $\frac{1}{2}^+$ octet baryon ground states $N(939)$, $\Lambda(1116)$, $\Sigma(1193)$, $\Xi(1318)$.
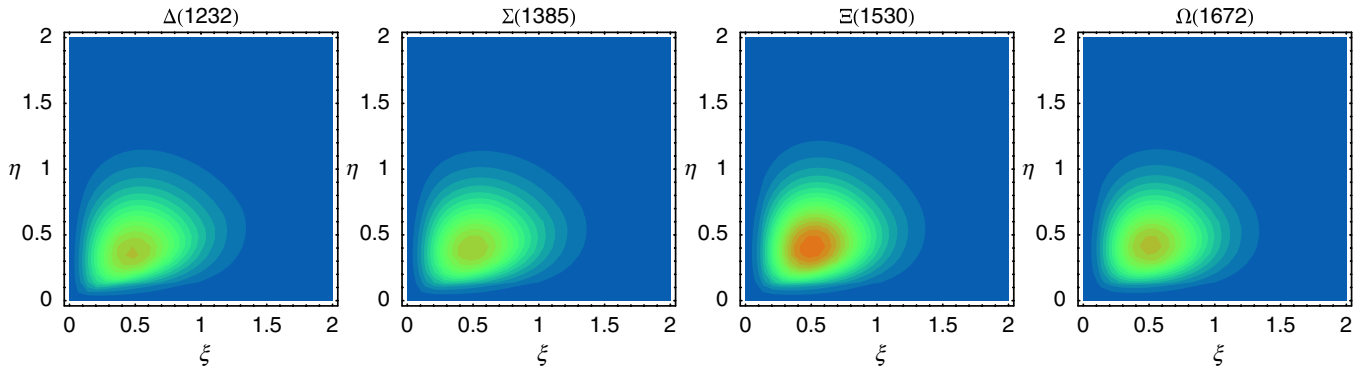

FIG. 6 (color online). Same as Fig. 5 for the $\frac{3}{2}^+$ decuplet baryon states $\Delta(1232)$, $\Sigma(1385)$, $\Xi(1530)$, $\Omega(1672)$.
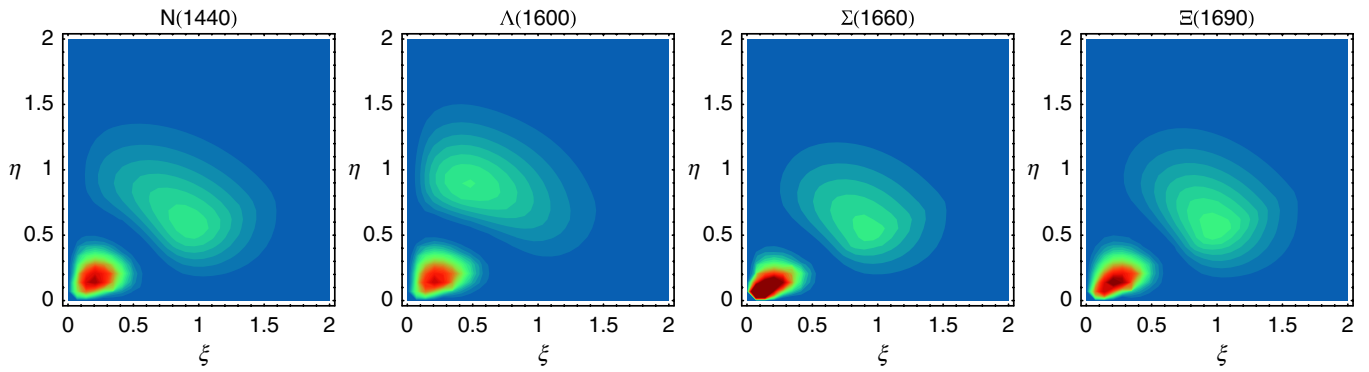

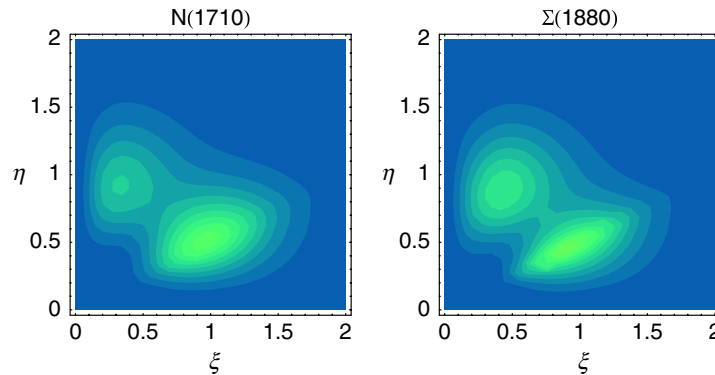FIG. 7 (color online). Same as Fig. 5 for the $\frac{1}{2}^+$ octet baryon states $N(1440)$, $\Lambda(1600)$, $\Sigma(1660)$, $\Xi(1690)$.

FIG. 8 (color online). Same as Fig. 5 for the $\frac{1}{2}^+$ octet baryon states $N(1710)$, $\Sigma(1880)$.
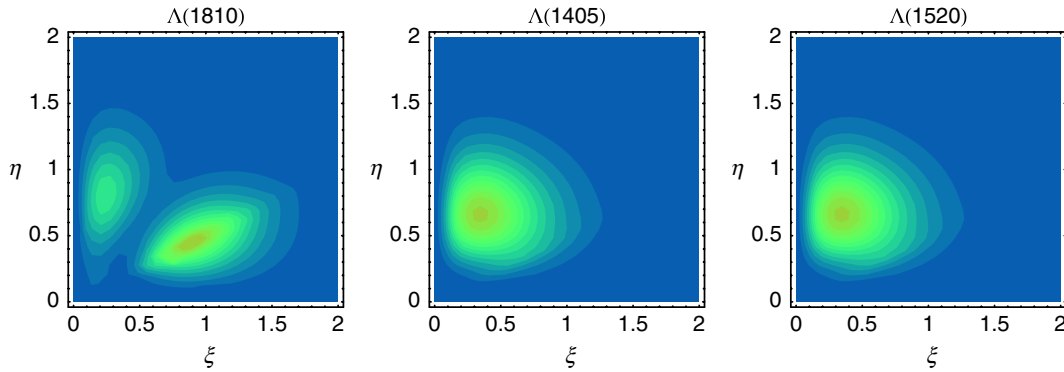
FIG. 9 (color online). Same as Fig. 5 for the $\frac{1}{2}^+$ singlet baryon state $\Lambda(1810)$, the $\frac{1}{2}^-$ singlet baryon state $\Lambda(1405)$, and the $\frac{3}{2}^-$ singlet baryon state $\Lambda(1520)$.

{QQQ} configurations, very probably because the mass value happens to lie so close to the NK threshold.

The next higher Λ eigenstate is an octet and it should thus be identified with the $\Lambda(1670)$ (see below). This reflects the typical behavior of the flavor singlet always lying lower than the octet as it is also found with the pairs of $\Lambda(1520)$ and $\Lambda(1690)$ and tentatively in the case of $\Lambda(1810)$.

7. Singlet: $\Lambda(1520)$

For the RCQMs used in this work the singlet states $\Lambda(1405)$ and $\Lambda(1520)$ are degenerate. Consequently, there is no difference between $J^P = \frac{1}{2}^-$ and $J^P = \frac{3}{2}^-$ with respect to baryon spectroscopy and the wave functions (see Fig. 9). However, when considering the decays, the distinct total angular momenta lead to other couplings and thus produce different results for the decay widths (cf. Figure 20 in the next section).

8. Octet: $N(1535)$, $\Lambda(1670)$, $\Sigma(1560)$

Into the next octet of excited states we assign the $N(1535)$, $\Lambda(1670)$, and $\Sigma(1560)$ resonances, which all have $J^P = \frac{1}{2}^-$. Only for the $\Lambda(1670)$ we find a sizable flavor singlet component, mixing this state with the

$\Lambda(1405)$. The spatial probability density distributions are shown in Fig. 10.

For the Σ member in this octet we advocate the experimentally measured $\Sigma(1560)$, which has only two-star status and is not considered in the PDG classification (cf. Table II). Our identification of the lowest $J^P = \frac{1}{2}^-$ Σ RCQM eigenstate, being a flavor octet, with $\Sigma(1560)$ is substantiated mainly by its decay properties [2]. Also, if this state becomes better established from experiment at this low energy, there is hardly another choice of placing it into a flavor multiplet.

The Ξ assignments in this multiplet must again be left open, as the possible remaining candidates seen in phenomenology, the $\Xi(1620)$ and maybe the $\Xi(2120)$, bear only one-star status and their J^P is not measured.

9. Octet: $N(1650)$, $\Lambda(1800)$, $\Sigma(1620)$

The next octet is the one with $J^P = \frac{1}{2}^-$ containing the $N(1650)$, $\Lambda(1800)$, and $\Sigma(1620)$ composed of $L = 1$ and $S = \frac{3}{2}$. They all exhibit a pure flavor octet content with no admixtures at all. The corresponding spatial probability density distributions are shown in Fig. 11.

For the Σ member of this octet it is suggested to choose the $\Sigma(1620)$, which has again only two-star status, however, with known $J^P = \frac{1}{2}^-$. This identification is further
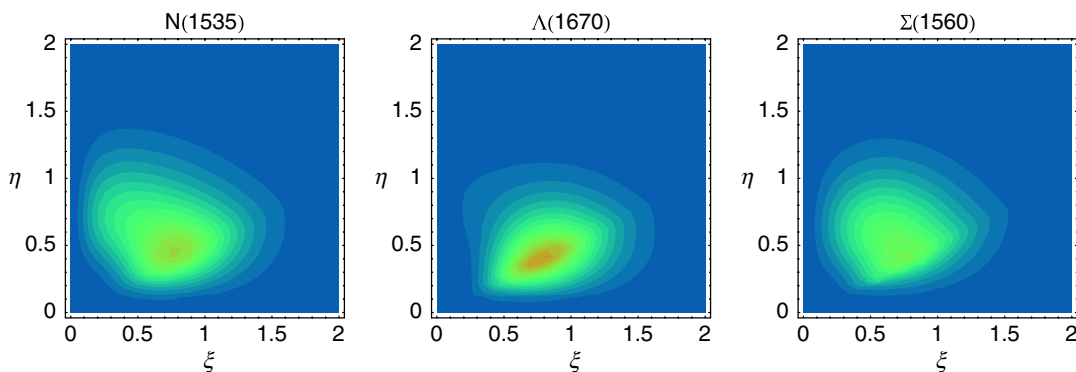

FIG. 10 (color online). Same as Fig. 5 for the $\frac{1}{2}^-$ octet baryon states $N(1535)$, $\Lambda(1670)$, $\Sigma(1560)$.
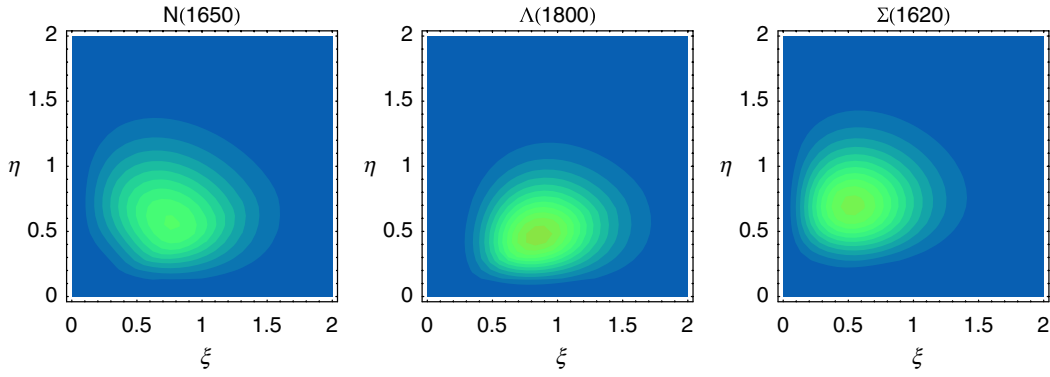
FIG. 11 (color online).   Same as Fig. 5 for the $\frac{1}{2}^{-}$ octet baryon states $N(1650)$, $\Lambda(1800)$, $\Sigma(1620)$.

motivated by the decay properties of the second excited octet Σ state with $J^{P} = \frac{1}{2}^{-}$ [2].

10. Octet: N(1520), Λ(1690), Σ(1670), Ξ(1820)

The $J^{P} = \frac{3}{2}^{-}$ octet with $N(1520)$ is completely filled with resonances experimentally established, namely, with $\Lambda(1690)$, $\Sigma(1670)$, and $\Xi(1820)$. The same classifications are suggested by the PDG and also by GP. In our RCQMs the $\Lambda(1690)$ is degenerate with the $\Lambda(1670)$ and thus also exhibits a sizable singlet admixture. The $N(1520)$ is a pure flavor octet, and the $\Sigma(1670)$ and $\Xi(1820)$ contain only

small decuplet components. The spatial probability density distributions of all of these resonances are shown in Fig. 12.

11. Octet: N(1700), Σ(1940)

For the $J^{P} = \frac{3}{2}^{-}$ octet involving $N(1700)$ we can at most classify the $\Sigma(1940)$ as a further member. This is in line with the classification by GP, while the PDG reports $\Sigma(1940)$ with $J^{P} = \frac{3}{2}^{-}$ but does not classify it into this octet nor into the decuplet with $J^{P} = \frac{3}{2}^{-}$. The latter would be an alternative possibility, and one must await further
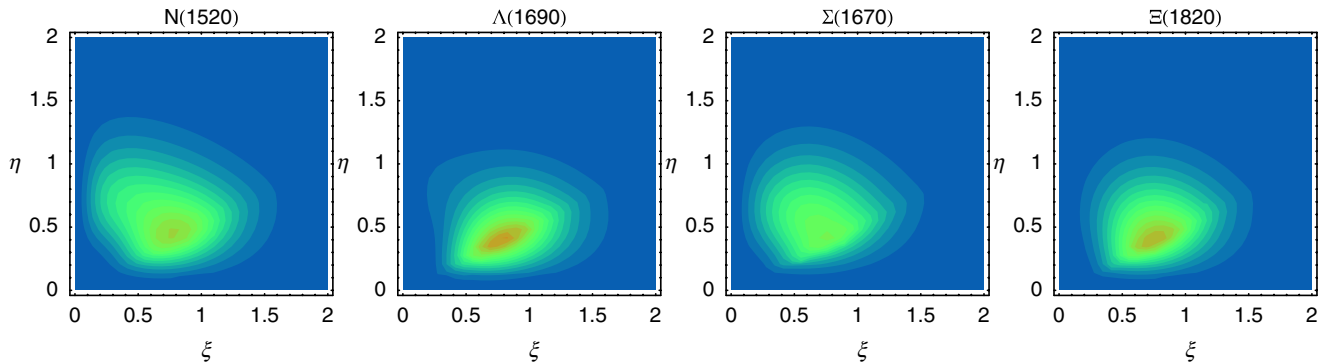

FIG. 12 (color online).   Same as Fig. 5 for the $\frac{3}{2}^{-}$ octet baryon states $N(1520)$, $\Lambda(1690)$, $\Sigma(1670)$, $\Xi(1820)$.
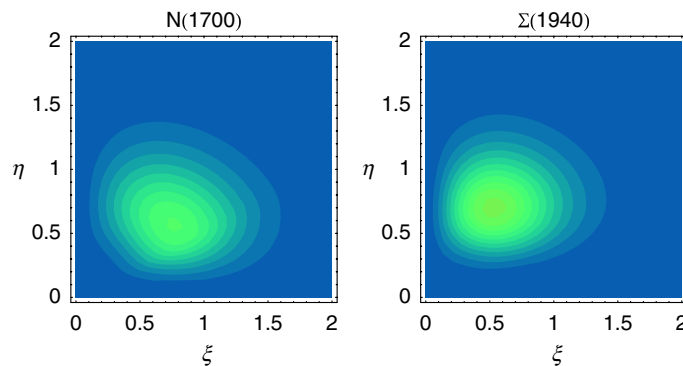

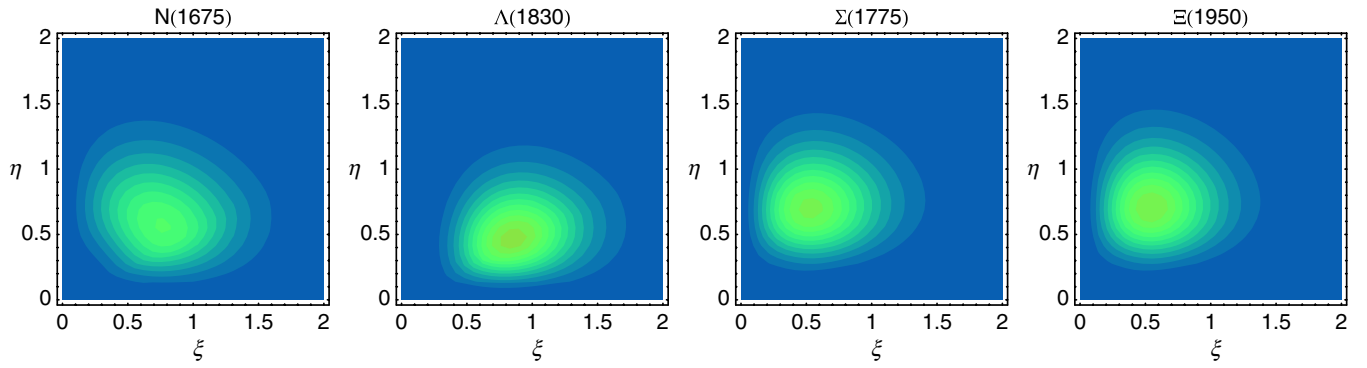FIG. 13 (color online).   Same as Fig. 5 for the $\frac{3}{2}^{-}$ octet baryon states $N(1700)$, $\Sigma(1940)$.

FIG. 14 (color online). Same as Fig. 5 for the $\frac{5}{2}^-$ octet baryon states $N(1675)$, $\Lambda(1830)$, $\Sigma(1775)$, $\Xi(1950)$.

experimental results, especially on the mesonic decays, for which no data have so far been reported by the PDG. For the Λ member of this octet there is no reliable experimental evidence, and the situation in the Ξ sector is similarly questionable. The spatial density distributions of the two states classified into this octet are demonstrated in Fig. 13.

12. Octet: $N(1675)$, $\Lambda(1830)$, $\Sigma(1775)$, $\Xi(1950)$

The $J^P = \frac{5}{2}^-$ octet with $L = 1$, $S = \frac{3}{2}$ is filled with the resonances $N(1675)$, $\Lambda(1830)$, $\Sigma(1775)$, and $\Xi(1950)$. All have 100% octet flavor content. GP arrive at the same classification, while the PDG does not include the $\Xi(1950)$. The latter is of unknown spin and parity, wherefore it could also be identified with another flavor multiplet. Because of its decay properties (to be discussed below) we suggest it to be a member of this octet. The spatial density distributions of all of these octet states are shown in Fig. 14.

13. Decuplet: $\Delta(1600)$, $\Sigma(1690)$

The $\frac{3}{2}^+$ decuplet with the $\Delta(1600)$ contains the first radial excitations above the decuplet ground states. We identify the $\Sigma(1690)$ to be a member of this decuplet. It has two-star status with unknown J^P. While GP arrive at the same classification, the $\Sigma(1690)$ is not considered by

the PDG. Given the classification of Σ resonances into octets as resulting from Table IV, it appears most natural to identify the $\Sigma(1690)$ with the first radial excitation of decuplet states. Both the $\Delta(1600)$ and $\Sigma(1690)$ have practically pure decuplet flavor content and their spatial probability density distributions are shown in Fig. 15. They exhibit the typical nodal behavior of first radial excitations (cf. the analogous octet states in Fig. 7).

14. Decuplet: $\Delta(1620)$, $\Sigma(1750)$

In the $\frac{1}{2}^-$ decuplet we have the $\Delta(1620)$ and $\Sigma(1750)$ resonances. Whereas the classification of $\Delta(1620)$ is beyond doubt, as it represents the lowest $\frac{1}{2}^-$ Δ excitation coming with $L = 1$ and $S = \frac{1}{2}$ (see Fig. 1), the identification of $\Sigma(1750)$ as a decuplet member depends on the classification of $\Sigma(1560)$ and $\Sigma(1620)$ as octet states. In the GBE RCQM only the third state of the $J^P = \frac{1}{2}^-$ excitations turns out to be a decuplet state. The mass eigenvalue fits best with the $\Sigma(1750)$ and it produces a decay width that falls into the general pattern established for relativistic results [2] (cf. also the discussion in the next section). Furthermore the classification of $\Sigma(1750)$ into this decuplet agrees with the one by GP. While the $\Delta(1620)$ is a pure flavor decuplet state, the $\Sigma(1750)$ bears a slight octet admixture. The spatial probability density
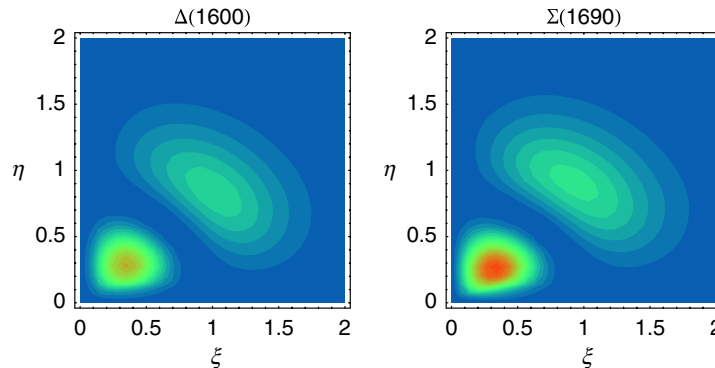

FIG. 15 (color online). Same as Fig. 5 for the $\frac{3}{2}^+$ decuplet baryon states $\Delta(1600)$, $\Sigma(1690)$.
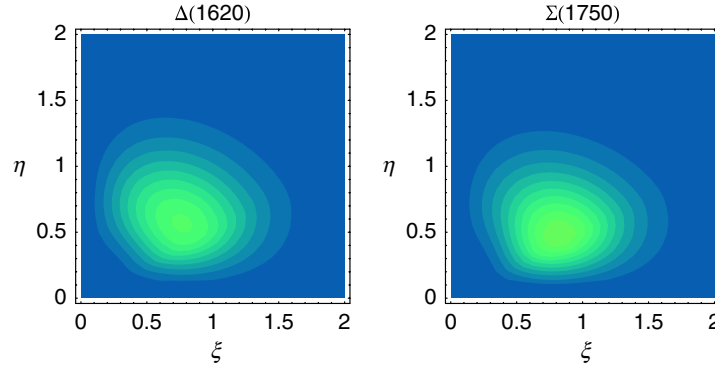
FIG. 16 (color online). Same as Fig. 5 for the $\frac{1}{2}^-$ decuplet baryon states $\Delta(1620)$, $\Sigma(1750)$.
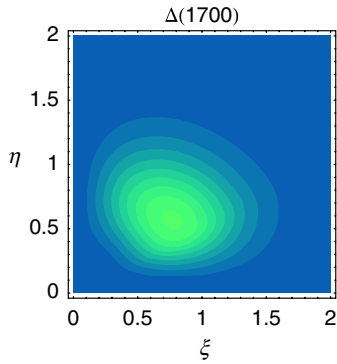

FIG. 17 (color online). Same as Fig. 5 for the $\frac{3}{2}^-$ decuplet baryon state $\Delta(1700)$.

distributions of the two members of this decuplet are depicted in Fig. 16.

15. Decuplet: $\Delta(1700)$

For the last decuplet one only has the $\Delta(1700)$ resonance with $J^P = \frac{3}{2}^-$ and $L = 1$, $S = \frac{1}{2}$. No other members of this decuplet are experimentally established firmly enough. The $\Delta(1700)$ is a pure flavor decuplet state and its spatial probability density distribution is plotted in Fig. 17.

VI. MESONIC DECAYS

The decay properties of the baryon resonances occurring in Tables IV, V, and VI are presented in Figs. 18–20. The covariant predictions for partial decay widths of all kind of decay modes are shown for both the GBE and OGE RCQMs.

We have chosen the same representation of the results as in Fig. 3 but here the experimental uncertainties of the decay widths as reported by the PDG are included too. Partial decay widths are not always available from experiment. In such cases we advocate the total decay widths and present the theoretical results of partial decay widths relative to them (shown by shaded lines without central values in the figures).

Beyond the relativistic results already published in Refs. [1–3] also the additional RCQM predictions for the two-star resonances of Table III are included in Figs. 18–20. In most cases the predictions of the GBE and OGE RCQMs are quite similar. If differences occur, they are in the first instance caused by resonance mass effects. The congruence of the results from the GBE and OGE RCQMs becomes even more pronounced, if experimental masses are employed instead of the theoretical ones. Only for certain decays wave-function effects are responsible too. The typical pattern that emerges is a general underestimation of the experimental data, with only a few exceptions.

The partial decay widths of the octet involving the $N(1440)$ resonance are given in the first column of Fig. 18. In the nonstrange sector there are only the π decays. Among them the most prominent decay $N(1440) \rightarrow N\pi$ is grossly underestimated by both RCQMs. In this case also the difference between the GBE and OGE RCQMs is sizable, even though it gets reduced, when mass effects are wiped out, i.e. when experimental masses are used instead of the theoretical ones [1]. The situation is quite similar for the $\Lambda(1600) \rightarrow \Sigma\pi$ decay and to some extent also for the $\Sigma(1660) \rightarrow \Sigma\pi$ and $\Sigma(1660) \rightarrow \Lambda\pi$ decays [2]. The decay width for the $\Xi(1690) \rightarrow \Xi\pi$ turns out to be very small, and we can only relate it to an experimental total width. Also the K decay widths follow the characteristic of remaining too small. The OGE RCQM results for $\Lambda(1600) \rightarrow NK$ and $\Xi(1690) \rightarrow \Sigma K$, which are relatively bigger, are dominated by mass effects. The corresponding decay widths get much reduced if the experimental masses are employed (see Ref. [3] and cf. Table III).

In the next octet we have only the decays of $N(1710)$ and $\Sigma(1880)$. It appears that the $N(1710) \rightarrow N\pi$ result contradicts the pattern usually found for the relativistic decay widths, as the theoretical prediction comes out large and relatively close to the (central value) of the experimental datum. However, it should be considered that the $N(1710)$, though being of three-star status, is not so safely established experimentally, as the various partial wave analyses do not agree very well [15]. In the case of the
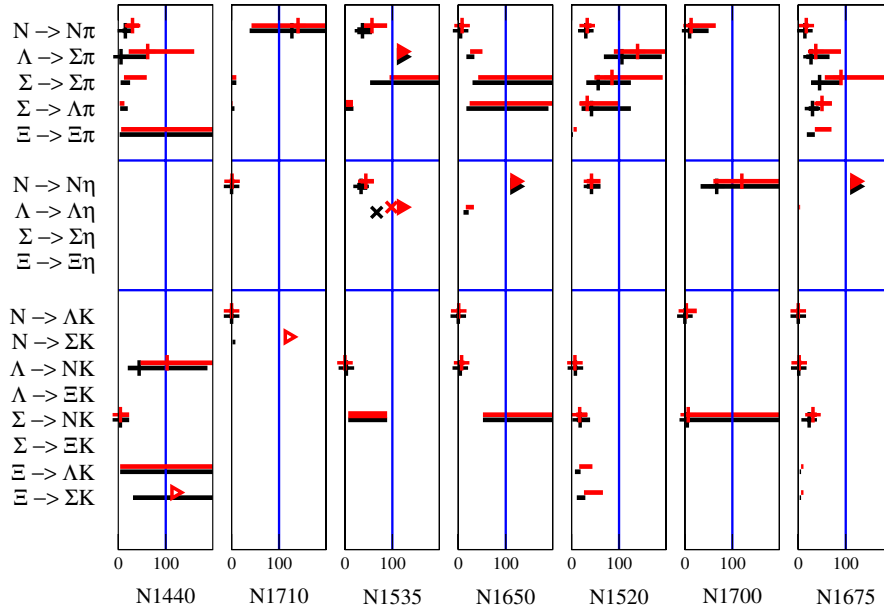
FIG. 18 (color online). Predictions for partial π, η, and K decay widths of the GBE (black/lower entries) and OGE (red/upper entries) RCQMs for the octets in Table IV from the PFSM calculation. The results shown by $+$ crosses are presented as percentages of the best estimates for experimental data reported by the PDG [15], with the horizontal lines showing the experimental uncertainties. In the case of shaded lines without crosses the PDG gives only total decay widths, and the theoretical results are represented relative to them. The triangles point to results outside the plotted range. For the particular decay $\Lambda(1670) \rightarrow \Lambda\eta$ in addition to the theoretical masses also experimental ones were used, and the corresponding results are marked by $\times$ crosses. For further explanations see the text.

strange decay the prediction of the OGE RCQM for the $N(1710) \rightarrow \Sigma K$ width is mainly caused by a threshold/mass effect. The large overshooting is essentially removed if the experimental mass is used [3]. For the $\Sigma(1880)$ all the π, η, and K decay widths are extremely small often compatible with zero (see Table III) and thus not even visible in Fig. 18.

In the octet involving the $N(1535)$ the $N \rightarrow N\pi$ and $N \rightarrow N\eta$ decays follow the usual pattern. For the $\Lambda(1670) \rightarrow \Sigma\pi$ decay both RCQMs predict a partial decay width much too large. The reason might be that the $\Lambda(1670)$ has a relatively big flavor singlet admixture of 28%. We note that a similar result is found for the $\Lambda(1690)$ resonance in the octet involving the $N(1520)$. The $\Lambda(1670) \rightarrow \Lambda\eta$ decay is rather sensitive to mass effects. In the case of the GBE RCQM the channel is closed, whereas for the OGE RCQM the prediction is too high. If the experimental masses are employed instead of the theoretical ones, both RCQMs produce a result close or slightly below the experimental width (cf. the $\times$ crosses in Fig. 18). The $\Lambda \rightarrow NK$ decay width turns out to be extremely small. In this octet we have in addition the $\Sigma(1560)$ decays, for which no estimates of experimental widths are given by the PDG. While the $\Sigma \rightarrow \Sigma\pi$ decay width might appear rather larger, the $\Sigma \rightarrow \Lambda\pi$ and $\Sigma \rightarrow NK$ widths come out quite small. This behavior suggests that the identification of the $J^P = \frac{1}{2}^-$ Σ eigenstate of this octet with the $\Sigma(1560)$ is the most reasonable choice. Further

experimental information on the decay properties of the $\Sigma(1560)$ would be highly welcome.

In the next octet the relativistic prediction for the $N(1650) \rightarrow N\pi$ decay width is again too small, while the one of $N(1650) \rightarrow N\eta$ comes out unusually large, as a notable exception [1]. The latter is true for both the GBE and OGE hyperfine interactions, and even in the case when experimental masses are used the situation is not changed. The $N(1650) \rightarrow \Lambda K$ decay width is again practically zero. For the $\Lambda(1800)$ an experimental partial width is only available for the strange NK decay channel. The theoretical prediction grossly underestimates the rather large $\Lambda \rightarrow NK$ width. The $\Lambda \rightarrow \Sigma\pi$ and $\Lambda \rightarrow \Lambda\eta$ widths can only be compared to the total Λ decay width and they result relatively small. Similarly, for the $\Sigma(1620)$ the decay widths can only be related to the total width. In this light the partial $\Sigma\pi$, $\Lambda\pi$, and NK decay widths appear to be relatively large, but we note that their sum still lies within the range of the total width. It is remarkable that among the above three channels the $\Sigma(1620) \rightarrow NK$ decay mode is the strongest one. In view of the reported data being rather old it would be desirable to have new measurements on the $\Sigma(1620)$.

For the octet with $N(1520)$ we have decays of all members including the Ξ. The partial widths of the π and η decays of $N(1520)$ are both predicted too small thus conforming to the typical pattern. The same appears to be true for the π and η decays of the strange resonances. The only
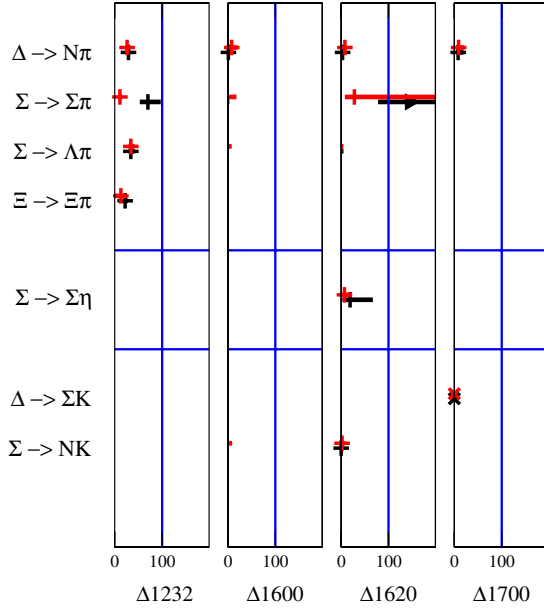
FIG. 19 (color online). Same as Fig. 18 but for the decuplets in Table V.

FIG. 20 (color online). Same as Fig. 18 but for the singlets in Table VI.

exception is the $\Lambda(1690) \to \Sigma\pi$ decay width coming out relatively large (and being in agreement with experiment). As in the case of $\Lambda(1670)$ the possible reason is again the considerable singlet admixture of 28%. On the other hand, the $\Lambda(1690) \to \Lambda\eta$ decay width is practically zero (and thus not visible in Fig. 18); there is no datum on that decay by the PDG. All the K decay widths are predicted too small by both RCQMs, where for the $\Xi(1820)$ no partial widths are reported by the PDG.

In the $J^P = \frac{3}{2}^-$ octet with $N(1700)$ the π decay widths are rather small, where in the case of the $\Sigma(1940)$ comparison is possible only to the total experimental width; because of its magnitude the small theoretical result is not visible in Fig. 18. Likewise the K decay widths are very small. For the $N(1700)$ only the ΛK width is available from phenomenology, while the ΣK width is not given. In this octet, only the $N(1700) \to N\eta$ width appears to be of considerable size but this is again an artifact of the representation in Fig. 18, as the experimental width is reported to be extremely small, practically consistent with zero.

In the last octet with $J^P = \frac{5}{2}^-$ we have all kinds of decay modes. The π decay widths are all too small. In the η channel only the decay width of $N(1675)$ is known from phenomenology. However, it is reported to be consistent with zero and thus the percentage of theoretical prediction falls outside the range plotted in Fig. 18. The η decay widths of $\Lambda(1830)$, $\Sigma(1775)$, and $\Xi(1950)$ are rather small, in some cases practically zero (and thus not visible in Fig. 18); the corresponding partial widths are not known from experiment. Similarly the K decay widths are all quite small, except for $\Sigma(1775) \to NK$. For the latter the experimental partial decay width is underestimated, like for the

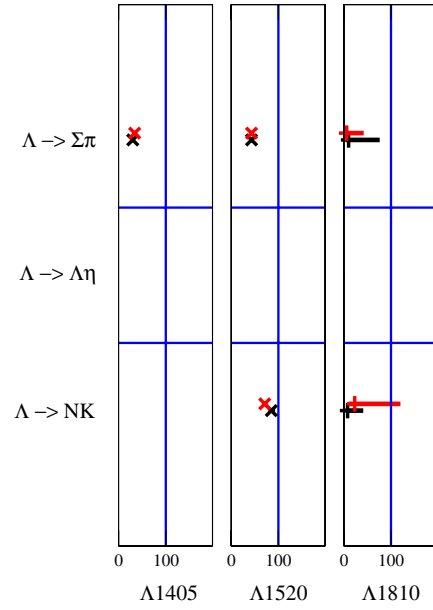two other decays $N(1675) \to \Lambda K$ and $\Lambda(1830) \to NK$, for which partial widths are reported from experiment.

For the lowest decuplet involving the $\Delta(1232)$ only π decays are possible. In all cases the theoretical results underestimate the experimental data. Only in the case of the GBE RCQM the prediction of the $\Sigma(1385) \to \Sigma\pi$ comes close to the experimental value. However, if experimental masses are used, the theoretical width is again reduced [2]. As a result the decay widths of this decuplet are quite consistent with the general pattern found for the relativistic quark-model predictions.

In the next decuplet with $\Delta(1600)$ we also have the $\Sigma(1690)$. The partial widths of all the possible decay modes of these radial-excitation states are found to be extremely small. Only for the $\Delta(1600) \to N\pi$ decay a partial width is reported from experiment. For the $\Sigma(1690) \to \Sigma\pi$, $\Sigma(1690) \to \Lambda\pi$, and $\Sigma(1690) \to NK$ we can only compare to the total width (see Table III).

The situation is quite similar for the decays in the next decuplet involving the $\Delta(1620)$. Here, we have the $\Sigma(1750)$, which bears a three-star status, and partial widths are available not only for the $\Sigma(1750) \to \Sigma\pi$ but also for the $\Sigma(1750) \to \Sigma\eta$ as well as $\Sigma(1750) \to NK$ decays. An exception to the typical pattern appears to be only the prediction for the partial width of the $\Sigma(1750) \to \Sigma\pi$ decay in the case of the GBE RCQM. The pertinent theoretical value falls within the error bars of the phenomenological width, which is reported to be rather small and could even be compatible with zero [15].

As a representative of the next decuplet with $J^P = \frac{3}{2}^-$ we only have the $\Delta(1700)$. Its π and K decay widths are again extremely small. For the latter we remark that the decay is

only possible if experimental masses are used. Both RCQMs predict the $\Delta(1700)$ mass too low (see Table I and/or Fig. 1).

Finally we consider the singlet decays in Fig. 20. As has already been stated in the previous section, the description of the $\Lambda(1405)$ poses a serious problem for all kinds of constituent quark models (relying on {QQQ} configurations only), as its mass cannot be reproduced in accordance with the experimental observation. It comes out at least 150–200 MeV too high for the RCQMs we consider here (see Fig. 2). These shortcomings have a big influence on the predictions for the π decay width; they come out way too big [2]. Therefore, we give in Fig. 20 the predictions obtained with the experimental masses. They fall below the experimental values and thus fit into the typical pattern.

Essentially, the same observations hold true for the next singlet, the $J^P = \frac{3}{2}^-$ $\Lambda(1520)$. Only we have here in addition the $\Lambda \rightarrow N\bar{K}$ channel open with the corresponding partial decay width reported from phenomenology. Both the π and K decay widths of this resonance are again predicted too small.

Finally, we have the $J^P = \frac{1}{2}^+$ singlet $\Lambda(1810)$. The dominant decays are to the π and K channels, which are of comparable strengths. The theoretical predictions underestimate both of them. The $\Lambda(1810) \rightarrow \Lambda\eta$ decay width comes out extremely small but different from zero; due to its smallness the corresponding entry is not visible in Fig. 20.

VII. CONCLUSIONS

We have presented a comprehensive study of the light and strange baryon resonances below ≈ 2 GeV in the framework of relativistic constituent quark models. In particular, we have considered their eigenvalue spectra and the properties of the eigenstates with regard to their spin-flavor contents and spatial structures. In addition we have explored the pattern of the predictions for the partial widths of the various mesonic decay modes. We have combined these findings to identify the theoretical eigenstates with experimental resonances and thus arrived at a new classification scheme for the known resonances into flavor multiplets. It has turned out that consideration of all of these evidences is required in order to produce a maximally reliable classification of the low-lying baryon resonances.

The relativistically invariant eigenvalue spectra have been obtained by the solution of the eigenvalue problem of the baryon mass operator using a stochastic variational method. Two different types of hyperfine interactions for a {QQQ} system of confined constituent quarks have been considered: the ones resulting from Goldstone-boson-exchange and from one-gluon-exchange dynamics, respectively. Their characteristic excitation spectra have been identified. By the solution of the eigenvalue problem, at the same time, the baryon eigenstates have been obtained.

Their configuration-space representations in the baryon rest frame (i.e. the baryon wave functions) have been analyzed considering their spin-flavor and spatial structures. Detailed evidences have thus been gained on the properties of the resonance eigenstates within each flavor multiplet with definite $(LS)J^P$ and certain radial excitation. The mixtures between flavor octet and singlet as well as octet and decuplet have been determined, and, for the first time, the characteristic spatial probability distributions for the ground and excited states have been shown. For the RCQMs considered here the spin-flavor and spatial structures of the baryon wave functions are qualitatively rather similar (cf. the examples shown in Fig. 4). In the discussion of the baryon properties in Sec. V we have therefore contented ourselves with presenting only the detailed results of the GBE RCQM. While the main conclusions do not depend on the type of RCQM considered, the distinct interactions present in either the GBE or OGE RCQM do lead to notable differences in the theoretical predictions.

Recently, first covariant predictions by RCQMs for mesonic decay widths of baryon resonances have become available [1–3,10,11]. The corresponding results provide additional insight for the classification of baryon resonances into flavor multiplets. Here, we have completed the theoretical results of decay widths for the GBE and OGE RCQMs regarding all baryon resonances below ≈ 2 GeV, with total orbital angular momentum $L < 2$, and at least two-star status. The evolving pattern shows that the experimental data for partial decay widths are in general underestimated. There are only a few notable exceptions, the $N(1710) \rightarrow N\pi$ decay, where the experimental situation can be considered as unsettled, the $\Lambda(1670) \rightarrow \Sigma\pi$ and the $\Lambda(1690) \rightarrow \Sigma\pi$ decays, where we have found considerable singlet admixtures, and the $N(1650) \rightarrow N\eta$ decay, where no convincing explanation is readily at hand.

Using all of these evidences a new classification of baryon ground states and resonances into flavor singlet, octet, and decuplet has been proposed. In most instances it is in accordance with the classification by the PDG [15] and also with the one by Guzey and Polyakov [34]. Only for the $\Lambda(1810)$ and for the $J^P = \frac{1}{2}^-$ octets and decuplets we find differences. Regarding the $\Lambda(1810)$ our classification differs from both of these schemes, as we identify this resonance as a flavor singlet. However, this is in agreement with the assignment suggested by Matagne and Stancu [40]. Contrary to the PDG but in accordance with Guzey and Polyakov, the $\Sigma(1560)$ and $\Sigma(1620)$ are placed into the $J^P = \frac{1}{2}^-$ octets involving the $N(1535)$ and the $N(1650)$, respectively. As a consequence, the $\Sigma(1750)$ is assigned to the decuplet involving the $\Delta(1620)$. Furthermore, we identify the $\Sigma(1940)$ as a member of the octet involving $N(1700)$ and the $\Sigma(1690)$ as a member of the decuplet involving the $\Delta(1600)$. In addition, we classify the $\Xi(1690)$ and the $\Xi(1950)$ into the octets involving the $N(1440)$ and $N(1675)$, respectively.

We remark that the suggested classification must also be considered with some caution. What regards theory, it is based on the description of the baryons as eigenstates of an invariant mass operator relying on {QQQ} degrees of freedom only. As this might not be adequate for resonances, it nevertheless constitutes a limitation for present methods of solving a relativistic few-quark problem. For the decay widths a restricted decay operator has been employed. Future works towards improving the relativistic description of baryons should primarily aim at extending the RCQMs to include additional degrees of freedom, like explicit couplings to decay channels. In such a framework, in particular, the resonant states will be generated more realistically.

Regarding phenomenology, sufficient experimental evidence is lacking for some Σ resonances and above all in the Ξ sector. For a complete assignment of states in the flavor octets additional information also on Λ resonances is urgently needed. In particular, determinations of J^P for the lesser known resonances and further measurements of the various partial decay widths would be highly welcome.

ACKNOWLEDGMENTS

[1] T. Melde, W. Plessas, and R. F. Wagenbrunn, Phys. Rev. C **72**, 015207 (2005); **74**, 069901(E) (2006).

[2] T. Melde, W. Plessas, and B. Sengl, Phys. Rev. C **76**, 025204 (2007).

[3] B. Sengl, T. Melde, and W. Plessas, Phys. Rev. D **76**, 054008 (2007).

[4] F. Stancu and P. Stassart, Phys. Rev. D **39**, 343 (1989).

[5] S. Capstick and W. Roberts, Phys. Rev. D **47**, 1994 (1993).

[6] P. Geiger and E. S. Swanson, Phys. Rev. D **50**, 6855 (1994).

[7] A. Krassnigg *et al.*, Few-Body Syst. Suppl. **10**, 391 (1999).

[8] W. Plessas *et al.*, Few-Body Syst. Suppl. **11**, 29 (1999).

[9] L. Theussl, R. F. Wagenbrunn, B. Desplanques, and W. Plessas, Eur. Phys. J. A **12**, 91 (2001).

[10] B. Metsch, in *Hadron Spectroscopy: Tenth International Conference*, edited by E. Klempt, H. Koch, and H. Orth, AIP Conf. Proc. No. 717 (AIP, New York, 2004), p. 646.

[11] S. Migura, Ph.D. thesis, University of Bonn, Bonn, Germany, 2007.

[12] D. Merten *et al.*, Eur. Phys. J. A **14**, 477 (2002).

[13] B. Metsch, U. Loering, D. Merten, and H. Petry, Eur. Phys. J. A **18**, 189 (2003).

[14] T. Melde and W. Plessas, arXiv:0711.0881.

[15] W.-M. Yao *et al.*, J. Phys. G **33**, 1 (2006).

[16] F. Cardarelli, E. Pace, G. Salme, and S. Simula, Phys. Lett. B **357**, 267 (1995).

[17] R. F. Wagenbrunn *et al.*, Phys. Lett. B **511**, 33 (2001).

[18] L. Y. Glozman *et al.*, Phys. Lett. B **516**, 183 (2001).

[19] S. Boffi *et al.*, Eur. Phys. J. A **14**, 17 (2002).

[20] T. Melde *et al.*, Phys. Rev. D **76**, 074020 (2007).

[21] K. Berger, R. F. Wagenbrunn, and W. Plessas, Phys. Rev. D **70**, 094027 (2004).

[22] B. D. Keister and W. N. Polyzou, Adv. Nucl. Phys. **20**, 225 (1991).

[23] P. Dirac, Rev. Mod. Phys. **21**, 392 (1949).

[24] H. Leutwyler and J. Stern, Ann. Phys. (N.Y.) **112**, 94 (1978).

[25] B. Bakamjian and L. H. Thomas, Phys. Rev. **92**, 1300 (1953).

[26] L. Y. Glozman, W. Plessas, K. Varga, and R. F. Wagenbrunn, Phys. Rev. D **58**, 094030 (1998).

[27] L. Y. Glozman *et al.*, Phys. Rev. C **57**, 3406 (1998).

[28] R. K. Bhaduri, L. E. Cohler, and Y. Nogami, Nuovo Cimento Soc. Ital. Fis. A **65**, 376 (1981).

[29] Y. Suzuki and K. Varga, *Stochastic Variational Approach to Quantum-Mechanical Few-Body Problems* (Springer-Verlag, Berlin, 1998).

[30] An alternative approach consists in solving the three-quark problem by Faddeev-type integral equations, which leads to identical results for the mass spectra [31].

[31] Z. Papp, A. Krassnigg, and W. Plessas, Phys. Rev. C **62**, 044004 (2000).

[32] We note that these two states have not been considered in Refs. [9,26] neither for fitting the parameters nor for the comparison of the theoretical results to the experimental data.

[33] N. P. Samios, M. Goldberg, and B. T. Meadows, Rev. Mod. Phys. **46**, 49 (1974).

[34] V. Guzey and M. V. Polyakov, arXiv:hep-ph/0512355.

[35] T. Melde, L. Canton, W. Plessas, and R. F. Wagenbrunn, Eur. Phys. J. A **25**, 97 (2005).

[36] A. LeYaouanc, L. Oliver, O. Pene, and J. C. Raynal, *Hadron Transitions in the Quark Model* (Gordon and Breach, New York, 1988).

[37] B. Sengl, Ph.D. thesis, University of Graz, Graz, 2006.

[38] B. Aubert *et al.*, arXiv:hep-ex/0607043.

[39] M. Pervin and W. Roberts, Phys. Rev. C **77**, 025202 (2008).

[40] N. Matagne and F. Stancu, Phys. Rev. D **74**, 034014 (2006).